Published in final edited form as:
J Biomech. 2008 ; 41(3): 595–602. doi:10.1016/j.jbiomech.2007.10.010.

Coronary Artery Flow Measurement Using Navigator Echo Gated Phase Contrast Magnetic Resonance Velocity Mapping at 3.0 Tesla

Kevin Johnson[a], **Puneet Sharma**[b], and **John Oshinski**[a,b,*]

[a]Department of Biomedical Engineering, Georgia Institute of Technology and Emory University, Atlanta, GA, USA

[b]Department of Radiology, Emory University, Atlanta, GA, USA

Abstract

A validation study and early results for noninvasive, *in vivo* measurement of coronary artery blood flow using phase contrast magnetic resonance imaging (PC-MRI) at 3.0 Tesla is presented. Accuracy of coronary artery blood flow measurements by phase contrast MRI is limited by heart and respiratory motion as well as the small size of the coronary arteries. In this study, a navigator-echo gated, cine phase velocity mapping technique is described to obtain time-resolved velocity and flow waveforms of small diameter vessels at 3.0 Tesla. Phantom experiments using steady, laminar flow are presented to validate the technique and show flow rates measured by 3.0 Tesla phase contrast MRI to be accurate within 15% of true flow rates. Subsequently, *in vivo* scans on healthy volunteers yield velocity measurements for blood flow in the right, left anterior descending, and left circumflex arteries. Measurements of average, cross-sectional velocity were obtainable in 224/243 (92%) of the cardiac phases. Time-averaged, cross-sectional velocity of the blood flow was 6.8±4.3 cm/s in the LAD, 8.0 ±3.8 cm/s in the LCX, and 6.0±1.6 cm/s in the RCA.

Keywords

MRI; fluid dynamics; coronary artery; human; CFD

INTRODUCTION

Determining coronary artery flow is important for both clinical and research applications. In clinical applications, reduced coronary flow reserve (the ratio of hyperemic to resting flow) has been shown to be an indicator of the ischemic significance of coronary lesions (Gould et al., 1990; Gould et al., 1974). Measurements of blood flow have also been used for the noninvasive detection of stenosis in coronary artery bypass grafts and recipient coronary arteries (Langerak et al., 2003). In research applications, determination of coronary flow is important in setting boundary conditions for computational fluid dynamics (CFD) studies of

*Corresponding author: John Oshinski, Ph.D., 1364 Clifton Rd, Atlanta, GA 30322, Email: jnoshin@emory.edu, Phone: (404)727-5894, Fax: (404)727-3887.

coronary hemodynamics (Gibson et al., 1993; Johnston et al., 2006; Perktold et al., 1998; Soulis et al., 2006).

Despite the high interest in determining coronary flow on a patient-specific basis, this has proved to be quite challenging. Most measures of coronary flow are either invasive and hence cannot be used unless clinically indicated (such as intravascular Doppler ultrasound), or lack the ability to accurately and reproducibly measure coronary flow (transesphogeal echocardigraphy), or are both invasive and not reproducible (thermodilution methods, angiographic grading).

Phase contrast magnetic resonance imaging (PC-MRI) is a technique which has been extensively used at 1.5 Tesla to determine blood velocity or flow within vessels such as the aorta, carotid arteries, and renal arteries (Bakker et al., 1995; Chatzimavroudis et al., 2001; Evans et al., 1993; Hoogeveen et al., 1998; Pelc et al., 1991; Rebergen et al., 1993). Few studies, however, have used PC-MRI to measure coronary flow due to; 1) the large degree of cardiac motion of the vessels, 2) the large amount and respiratory motion of the vessels, and 3) the small diameter of the vessels. Cardiac motion effects are mitigated by gating the acquisition to the R-wave on the electrocardiograph (ECG) signal. Most previous studies examining coronary flow have employed breath-holding to reduce respiratory coronary motion effects. However, in a recent study, one-third of patients were unable to hold their breath suitably for high resolution cardiac MR imaging during a breath-hold PC-MRI measurement (Jahnke et al., 2006). Use of a breath-hold technique also requires a rapid scan which in turn limits spatial or temporal resolution.

Navigator echo gating is a technique that allows image acquisition during free breathing. A small excitation pulse is positioned over the diaphragm and monitors the patient's breathing – only allowing data acquisition during end-expiration (Figure 1, Oshinski et al., 1996). Navigator echo gating has recently been incorporated with PC-MRI for measuring velocity of the myocardium during cardiac contraction and relaxation (Delfino et al., 2006) and for the assessment of three-dimensional blood flow in the aorta (Markl et al., 2007).

Accuracy of PC-MRI can be limited in small vessels due to undersampling of velocity measurements across the vessel and by partial volume effects at the vessel wall caused by insufficient spatial resolution (Hoogeveen et al., 1998; Tang et al., 1993). Improvements in spatial resolution and signal-to-noise ratio (SNR) for cardiac imaging applications can be achieved by using higher field strength 3.0 Tesla scanners (Gutberlet et al., 2006; Gutberlet et al., 2004). Validation studies of 3.0 Tesla PC-MRI in larger diameter vessels have recently been performed showing good precision and accuracy at high flow rates (Lotz et al., 2005). However, the accuracy of navigator echo gated 3.0 Tesla PC-MRI for low flow rates in small diameter vessels, as is seen in coronary artery flow, is unknown.

In this study, we evaluated the use of navigator echo gated PC-MRI at 3.0 Tesla in a flow phantom under controlled flow conditions and subsequently applied the technique to obtain velocity waveforms of the proximal left anterior descending (LAD), left circumflex (LCX), and right coronary arteries (RCA) in healthy volunteers. Our hypothesis is that phase contrast imaging, when combined with navigator echo gating, is a capable technique for measuring flow in small diameter blood vessels such as the coronary arteries. The purpose of the study was to: 1) evaluate the accuracy of navigator echo gated, 3.0 Tesla PC-MRI in an *in vitro* phantom study with respiratory motion and flow rates representative of the coronary arteries, and 2) apply the technique in a series of volunteers to obtain *in vivo* measurements of coronary blood flow in the left anterior descending (LAD), left circumflex (LCX), and right coronary arteries (RCA).

METHODS

Phantom Model

The coronary model used was a 4.0 mm diameter, non-compliant plastic tube. The tubing was placed on top of a left ventricle phantom model consisting of two concentric Plexiglas cylinders filled with polyvinyl alcohol cryogel (PVA) to simulate myocardium. Steady, laminar flow through the model was provided by a variable speed flow pump (CardioFlow 1000, Shelley Medical Systems, Toronto, Canada) at programmed rates of 2.00 ml/s, 2.25 ml/s, and 2.50 ml/s to simulate a range of coronary artery flow rates and velocities. These flow rates corresponded to time-averaged, cross sectional velocities of 15.9 – 19.9 cm/s through the 4 mm tubing.

Respiratory motion in the phantom was provided by an animal respirator (Harvard Apparatus, Holliston, MA, USA) which was attached to an inflatable bag placed under the ventricular phantom. The respirator inflated and deflated the bag at a rate of 10 cycles/minute with an excursion of 15–20 mm at the center of the model typical of cardiac and respiratory motion (Wang et al., 1995). The circulating fluid was a 60% glycerin, 40% water mixture designed to approximate the viscosity and T1 properties of blood. Bags of saline were positioned around the phantom to simulate static tissue (Figure 2). Flow rates determined from the MR images were compared with flow measured by timed collection of the pump's output during the scan in a graduated cylinder.

In-Vitro Phantom Imaging Protocol

All scans were performed on a Philips Medical Systems Intera 3.0 Tesla scanner equipped with a 5-element cardiac phased array coil (Phillips Medical Systems, Best, The Netherlands). For the phantom studies, a single slice plane was oriented perpendicular to the plastic tubing for velocity measurements. The PC-MRI scan sequence used for these studies was a segmented FLASH sequence (3 lines/segment), with flow encoded and non-encoded images acquired in separate heartbeats. Other imaging parameters were: 256 mm^2 FOV, 256×256 matrix, 1 mm × 1mm in-plane resolution, 4 mm slice thickness, TR/TE/α = 7.0/3.5/15. Velocity was measured in the through-plane direction using a velocity encoding value (VENC) of 40 cm/s. Temporal resolution of the scan was 50 ms. A 60 beats per minute physiology simulator was used to acquire velocity data at 17 temporal phases, prospectively gated. The acquisition and processing of the navigator echo at the start of each simulated phase prevents data acquisition during the first 132 ms of each cycle, hence there are 17 acquired phases rather than 20 during a 60 beats per minute simulation. The navigator echo was placed over the ventricle phantom and monitored the simulated respiratory motion at the start of each heartbeat. When the air-PVA interface was within 2 mm of the peak displacement, data from that simulated cardiac cycle was accepted; otherwise the phase encoding step is skipped until the boundary falls within the navigator window. Background phase correction was performed by standard methods (Walker et al., 1993). To assess repeatability, a total of 36 flow scans were acquired (14 scans at 2.0 and 2.5 ml/s, 8 scans at 2.25 ml/s) over multiple imaging sessions. The true flow rate was measured by collecting the fluid in a graduated cylinder over the course of each scan. The total volume collected was divided by the scan time and cross-sectional area of the tubing to determine the time-average cross-sectional velocity for comparison with the PC-MRI measurements.

The PC-MR images were transferred to a dedicated workstation and evaluated using the FLOW software package (AZL, Lieden, The Netherlands, van der Geest et al., 1998). Regions-of-interest (ROIs) were manually drawn for each cardiac phase using the magnitude images and then copied to the velocity encoded images on each of the time frames. The average ROI size was 21 pixels, or 23 mm^2, and included the tubing wall in an attempt to include velocity measurements from any partial volume pixels. The program then averages the velocity values

for all pixels within the ROI. Values of time-average cross-sectional velocity (cm/s) for each time point were exported to a spreadsheet for comparison and analysis. Since only gross, or average, flow and not instantaneous flow could be verified by timed collection, velocities calculated at different phases of the PC-MRI acquisition were averaged to arrive at a final velocity measurement for each scan. The difference between flow velocity measurements calculated by PC-MRI and by timed collection was analyzed as root mean squared (RMS) error: $\mathrm{RMS}=\frac{\sum \sqrt{(\mathrm{flow}_{\mathrm{collection}} - \mathrm{flow}_{\mathrm{PC-MR}})^2}}{N}$. This parameter retains the magnitude of the difference but not the sign such that positive and negative errors do not average out.

In Vivo Imaging Protocol

Coronary artery blood flow was measured in nine volunteers (2 female, 7 male; age 22–38) with no previous history of cardiovascular disease in a total of 16 coronary vessels (6 RCA, 6 LAD, 4 LCX). Informed consent was obtained prior to MRI scans and the study was approved by the university's Institutional Review Board (IRB). To plan the flow measurements, a transverse stack of 35–40 slices was acquired over the heart using a navigator echo gated 3D "whole heart" coronary MR angiography sequence which has been described previously (Weber et al., 2003). Briefly, image acquisition was gated to the ECG signal and occurred in mid-to-late diastole during the quiescent period of the cardiac cycle. The navigator echo was placed over the right hemi-diaphragm and was acquired at the start of each cardiac cycle. Total imaging time for the axial MRA stack was approximately 3 minutes during free breathing. From the transverse stack, a scan plane was selected which passed through the coronary ostium and points in the mid and distal regions for each of the left anterior descending, left circumflex or the right coronary artery. The same navigator echo gated MRA sequence was used in the double oblique plane with 10 slices to ensure visualization of the vessel in the imaging plane. Example images from one volunteer are shown in Figure 3. Once the target artery was localized in-plane, a navigator echo gated PC-MRI scan was positioned perpendicular to a straight region of the coronary artery at a location (mean ± SD) of 2.6±1.3 cm from the ostia of the RCA at the aorta, 3.0±1.2 cm from the aorta along the LAD and 3.4±0.4 cm along the LCX – making sure the LAD and LCX scans were located distal to the left coronary artery bifurcation. Spatial resolution for the PCMR scan was 1mm × 1mm in-plane with 4 mm through-plane slice thickness. Velocity was encoded only in the through-plane direction using a VENC of 35 cm/s. The PCMR sequence described for the phantom study was implemented and velocity was acquired for 11–19 cardiac phases, depending on the subject's heart rate. While the temporal resolution of this scan was 50 ms, the inclusion of the navigator echo pulse prevents velocity data acquisition for the first 132 ms. Imaging time required for one PC-MRI scan ranged from approximately 4 to 10 minutes depending on the heart rate and navigator efficiency of the subject. In order to keep total exam time under 45 minutes, most scanning sessions resulted in the evaluation of two arteries. Repeat examinations were required to evaluate the third artery. Variant coronary anatomies such as a left main artery trifurcation and a very tortuous LCX prevented evaluation of those arteries in two subjects.

Flow measurements were evaluated using the FLOW software package as described previously. Rather than only measuring velocity in four central pixels as has previously been done at 1.5 Tesla (Keegan et al., 2004), ROIs were drawn to include as much of the vessel cross-section as possible. Average ROI areas with standard deviations were 6.9±1.9 pixels in the LAD, 5.0±1.2 pixels in the LCX, and 8.5±2.7 pixels in the RCA.

RESULTS

Phantom Model Studies

Velocity measurements in the phantom model made with the navigator echo gated PC-MRI sequence showed moderate agreement with values obtained with timed collections at all flow rates (Table 1). Root mean squared (RMS) error in flow measurements over all imaging sessions was 15% and did not exceed 20% for any flow rate during any session. A Bland-Altman plot showing errors for each scan is shown in Figure 4.

Volunteer *In Vivo* Coronary Flow Studies

MR angiographic images of the coronaries and phase velocity images of LAD, LCX, and RCA flow were successfully obtained in all subjects (Figure 3). Coronary artery blood flow velocity was measurable in 62/79 total cardiac phases of LAD flow, 51/51 phases of LCX flow, and 111/113 phases of RCA flow – 224/243 overall (92%). Flow in the remaining phases was not measurable due either to blurring from motion artifact or the vessel's proximity to the ventricular blood pool.

Time-averaged cross-sectional velocity over all subjects was 6.0±1.6 cm/s in the RCA, 6.8±4.3 cm/s in the LAD, and 8.0±3.8 cm/s in the LCX. Time-average flow rates were 37.7±19.0 ml/min in the RCA, 29.7±17.4 ml/min in the LAD, and 28.4±19.7 ml/min in the LCX. Examples of cross sectional velocity curves for the LAD, LCX, and RCA of selected subjects are shown in Figure 5.

DISCUSSION

This study evaluated the use of navigator echo gated PC-MRI at 3.0 Tesla for measuring blood flow in the proximal coronary arteries. The major findings of the study were:

1. An *in-vitro* phantom study measuring flow at typical coronary artery flow rates demonstrated an RMS error of 15% for PC-MRI flow measurements.
2. *In vivo* implementation of the navigator echo PC-MRI technique in the RCA, LAD, and LCX arteries yielded measurable velocities scans in 92% of total cardiac phases.
3. Time-averaged velocity of the blood flow was 6.8±4.3 cm/s in the LAD, 8.0±3.8 cm/s in the LCX, and 6.0±1.6 cm/s in the RCA.

In vitro Study

Lotz et al., (2005) has shown that 3.0 Tesla PC-MRI can be used to measure flow with a high degree of accuracy and precision in large diameter phantom vessels. Their study reported an average error of 0.6% ± 0.6% for a range of flow rates between 480 and 1320 ml/min in flow phantoms with inner diameter greater than 10 mm. Repeated measurements of a single flow rate resulted in deviations of 0.1%. This study, however, did not report individual flow rate values for the various tube sizes so average cross-section velocities are not known flow rates. The larger errors seen in our study indicate that spatial resolution remains a limiting factor in the accuracy of PC-MRI flow measurements in small diameter vessels. A previous *in vitro* study of 1.5 Tesla small vessel PC-MRI concluded that 16 pixels or more are needed across the diameter of a vessel in order to consistently measure flow rates accurate to within 10% (Tang et al., 1993). This resolution allows measurement of the velocity profile across the vessel and accurate description of the peak velocities seen at the centerline of parabolic tube flow. Flow measurements with a pixel-to-diameter ratio less than 16 tend to underestimate peak velocities and can also be affected by partial-volume artifacts at the vessel wall. However, flow measurements are less affected by the poor spatial resolution. This is because the velocity

measurement represents an average of the velocities within the pixel while flow is calculated as average velocity in a pixel times the area of the pixel.

Other sources of error in our phantom study include electronic noise generated by the pump, background phase errors, or effects of inhomogeneities or gradient eddy currents in the magnetic field that are not fully corrected by linear or planar algorithms used in clinical scanners and reconstruction software (Bernstein et al., 1998; Gatehouse et al., 2005). Higher field strengths are more sensitive to magnetic field inhomogeneities and susceptibility artifacts. However, these errors are secondary to the spatial resolution issues.

In vivo Coronary Artery Study

Previous studies of breath-hold PC-MRI at 1.5 Tesla have presented varying results for velocities and flow rates in the coronary arteries. In an investigation of the effect of cardiac motion on flow assessment, Hofman et al., 1996 found time-averaged velocity in six healthy subjects was 7±2 cm/s and volume flow was 30±10 ml/min in the RCA. Another study of eight healthy volunteers presented mean flow rates (cross sectional velocities were not reported) of 59±15 ml/min in the LAD and 38±10 ml/min in the RCA (Marcus et al., 1999). Our results fall within the range of these earlier findings. The navigator echo PC-MRI sequence used in this study is free-breathing and has the advantage of allowing better resolution and can be used in patients that may be noncompliant or unable to hold their breath repeatedly at the same location or for extended periods of time.

Peak blood flow rate in the RCA occurred predominantly in early to mid diastole as the surrounding myocardium relaxed after systolic contraction. A similar tendency was also observed for flow in the LAD and LCX. In the coronary vessels, the surrounding myocardium contracts during systole raising the pressure in the coronary arteries, decreasing the pressure gradient between the aorta and the coronary arteries and restricting coronary blood flow until the myocardium relaxes during diastole (Berne et al., 1997). Inter-subject variations in the pattern and amplitude of velocity curves as well as differences in heart rate, however, prevented broader characterizations of blood flow across the subject population.

Schiemann et al., 2006 measured velocity in the LCA and RCA of eighty-three patients without coronary artery disease using PC-MRI at 1.5 Tesla and found 61% of the vessels to have a biphasic velocity pattern. The remaining velocity curves were monophasic or demonstrated reduced fluctuation nearing steady velocities. Peak velocities were measured for each patient with 25 – 75% quartiles of 16 – 30 cm/s in the LCA and 10 – 18 cm/s in the RCA. This variability in both velocity waveform characterization and peak velocity was also observed in our study and suggests that a velocity curve averaged over many patients or obtained from previous literature may be insufficient for accurate CFD modeling of patient-specific coronary flow or wall shear stress.

Navigator echo gated PCMR at 3.0 Tesla has potential for use in setting inflow velocity boundary conditions for patient-specific computational fluid dynamics (CFD) simulations of coronary blood flow. Patient-specific CFD models are desirable due to a large degree of physiologic variability in the human population and interest in the relationship between wall shear stress and arterial disease. Past computational models of coronary blood flow have used a variety of flow boundary conditions. Ramaswamy et al., 2004 found that the impact of using pulsatile flow in lieu of steady flow on WSS calculations for the LAD was minimal; but the use of steady flow boundary conditions prevents the study of other parameters such as oscillating shear index and WSS angle deviation. In their *in vitro* study of curvature dynamics' influence on coronary flow, Prosi et al., 2004 used an (invasively-determined) LAD flow curve specific to the subject upon which their geometric model was based. For a similar study, Pivkin et al., 2005 used a sinusoidal velocity waveform. Other investigations have defined steady state

boundary conditions (Soulis et al., 2006) or used a reference waveform from previous literature (Frauenfelder et al., 2007; Glor et al., 2003; Johnston et al., 2006). Few studies have paired *in vivo* geometries with corresponding *in vivo* flow.

This study used a 3.0T MRI scanner. Although we did not perform a direct comparison between 1.5 Tesla and 3.0 Tesla, other studies have shown improvement in SNR at 3.0 Tesla (Gutberlet et al., 2006; Gutberlet et al., 2004; Lotz et al., 2005; Wittlinger et al., 2005). This increase in SNR from 1.5 Tesla to 3.0 Tesla can be bartered to improve either spatial resolution or temporal resolution as desired for a given application. Other pulse sequences, such as SSFP based flow techniques (Markl et al., 2003), might also be adapted for 3.0 PCMR velocity measurements and yield improvements over 1.5 imaging.

Several limitations to our study must be acknowledged. First, the steady flow conditions simulated for the *in vitro* study are not accurate representations of coronary artery blood flow. Time-resolved, pulsatile flow would provide a better simulation of the *in vivo* condition. The nature of MRI velocity measurement is the same whether the flow is steady or unsteady, and the accuracy of PC-MRI at 1.5T in measuring unsteady flow has been previously established (Arheden et al., 2001; Frayne et al., 1995). Similarly, the incorporation of cardiac motion to the *in vitro* phantom in addition to respiratory motion would be an improvement to our model. The combination of repeatable cardiac and respiratory motion is prohibitively complex due to the necessity of keeping metallic components and electronic equipment out of the field of the MRI scanner. We chose to simulate respiratory motion to evaluate the navigator echo sequence since cardiac motion is largely conquered by ECG gating.

While the flow rates observed in the *in vivo* study are lower than those used for the *in vitro* evaluation, the *in vivo* velocities are very similar to those of the *in vitro* scans (16–20 cm/s *in vitro* vs. 6–23 cm/s *in vivo*). However, a difference in the intrinsic error of the *in vitro* velocity measurements cannot be ruled out due to the use of a different velocity encoding value.

While the use of navigator echo gating improves image quality, the inability to collect a full temporal dataset over the cardiac cycle is a limitation for CFD applications. The navigator executes over 132 ms, so flow in that part of the cardiac cycle can not be measured. These limitations might be lessened by future improvements in the time required to create the gating algorithm – such as gating during one heart beat and acquiring a full dataset in the next heart beat, assuming minimal respiratory motion during two sequential heart beats. This could potentially double scan time; but would result in velocity data for the entire cardiac cycle.

In conclusion, free-breathing, navigator echo gated, quantitative phase velocity mapping at 3.0 Tesla is a promising tool for non-invasive measurements of *in vivo* blood flow in the coronary arteries. With further development and optimization, this technique has potential for further clinical use in determining coronary flow reserve as well as research applications such as providing patient-specific boundary conditions for hemodynamic simulations.

Acknowledgements

We would like to thank Dr. Steven Lloyd for providing scanner time at the University of Alabama at Birmingham. This study was supported by National Institutes of Health BRP grant HL70531.

References

Arheden H, Saeed M, Tornqvist E, Lund G, Wendland MF, Higgins CB, Stahlberg F. Accuracy of segmented MR velocity mapping to measure small vessel pulsatile flow in a phantom simulating cardiac motion. J Magn Reson Imaging 2001;13:722–728. [PubMed: 11329193]

Bakker CJ, Kouwenhoven M, Hartkamp MJ, Hoogeveen RM, Mali WP. Accuracy and precision of time-averaged flow as measured by nontriggered 2D phase-contrast MR angiography, a phantom evaluation. Magn Reson Imaging 1995;13:959–965. [PubMed: 8583874]

Berne, RM.; Levy, MN. Cardiovascular Physiology. Vol. 7th edition. St. Louis: Mosby-Year Book; 1997.

Bernstein MA, Zhou XJ, Polzin JA, King KF, Ganin A, Pelc NJ, Glover GH. Concomitant gradient terms in phase contrast MR: analysis and correction. Magn Reson Med 1998;39:300–308. [PubMed: 9469714]

Chatzimavroudis GP, Oshinski JN, Franch RH, Walker PG, Yoganathan AP, Pettigrew RI. Evaluation of the precision of magnetic resonance phase velocity mapping for blood flow measurements. J Cardiovasc Magn Reson 2001;3:11–19. [PubMed: 11545135]

Delfino JG, Bhasin M, Cole R, Eisner RL, Merlino J, Leon AR, Oshinski JN. Comparison of myocardial velocities obtained with magnetic resonance phase velocity mapping and tissue Doppler imaging in normal subjects and patients with left ventricular dyssynchrony. J Magn Reson Imaging 2006;24:304–311. [PubMed: 16786564]

Evans AJ, Iwai F, Grist TA, Sostman HD, Hedlund LW, Spritzer CE, Negro-Vilar R, Beam CA, Pelc NJ. Magnetic resonance imaging of blood flow with a phase subtraction technique. In vitro and in vivo validation. Invest Radiol 1993;28:109–115. [PubMed: 8444566]

Frauenfelder T, Boutsianis E, Schertler T, Husmann L, Leschka S, Poulikakos D, Marincek B, Alkadhi H. In-vivo flow simulation in coronary arteries based on computed tomography datasets: feasibility and initial results. Eur Radiol 2007;17:1291–1300. [PubMed: 17061068]

Frayne R, Steinman DA, Ethier CR, Rutt BK. Accuracy of MR phase contrast velocity measurements for unsteady flow. J Magn Reson Imaging 1995;5:428–431. [PubMed: 7549205]

Gatehouse PD, Keegan J, Crowe LA, Masood S, Mohiaddin RH, Kreitner KF, Firmin DN. Applications of phase-contrast flow and velocity imaging in cardiovascular MRI. Eur Radiol 2005;15:2172–2184. [PubMed: 16003509]

Gibson CM, Diaz L, Kandarpa K, Sacks FM, Pasternak RC, Sandor T, Feldman C, Stone PH. Relation of vessel wall shear stress to atherosclerosis progression in human coronary arteries. Arterioscler Thromb 1993;13:310–315. [PubMed: 8427866]

Glor FP, Long Q, Hughes AD, Augst AD, Ariff B, Thom SA, Verdonck PR, Xu XY. Reproducibility study of magnetic resonance image-based computational fluid dynamics prediction of carotid bifurcation flow. Ann Biomed Eng 2003;31:142–151. [PubMed: 12627821]

Gould KL, Kirkeeide RL, Buchi M. Coronary flow reserve as a physiologic measure of stenosis severity. J Am Coll Cardiol 1990;15:459–474. [PubMed: 2137151]

Gould KL, Lipscomb K, Hamilton GW. Physiologic basis for assessing critical coronary stenosis. Instantaneous flow response and regional distribution during coronary hyperemia as measures of coronary flow reserve. Am J Cardiol 1974;33:87–94. [PubMed: 4808557]

Gutberlet M, Noeske R, Schwinge K, Freyhardt P, Felix R, Niendorf T. Comprehensive cardiac magnetic resonance imaging at 3.0 Tesla: feasibility and implications for clinical applications. Invest Radiol 2006;41:154–167. [PubMed: 16428987]

Gutberlet M, Spors B, Grothoff M, Freyhardt P, Schwinge K, Plotkin M, Amthauer H, Noeske R, Felix R. Comparison of different cardiac MRI sequences at 1.5 T/3.0 T with respect to signal-to-noise and contrast-to-noise ratios - initial experience. Rofo 2004;176:801–808. [PubMed: 15173972]

Hofman MB, van Rossum AC, Sprenger M, Westerhof N. Assessment of flow in the right human coronary artery by magnetic resonance phase contrast velocity measurement: effects of cardiac and respiratory motion. Magn Reson Med 1996;35:521–531. [PubMed: 8992202]

Hoogeveen RM, Bakker CJ, Viergever MA. Limits to the accuracy of vessel diameter measurement in MR angiography. J Magn Reson Imaging 1998;8:1228–1235. [PubMed: 9848733]

Jahnke C, Paetsch I, Achenbach S, Schnackenburg B, Gebker R, Fleck E, Nagel E. Coronary MR imaging: breath-hold capability and patterns, coronary artery rest periods, and beta-blocker use. Radiology 2006;239:71–78. [PubMed: 16493014]

Johnston BM, Johnston PR, Corney S, Kilpatrick D. Non-Newtonian blood flow in human right coronary arteries: transient simulations. J Biomech 2006;39:1116–1128. [PubMed: 16549100]

Keegan J, Gatehouse PD, Mohiaddin RH, Yang GZ, Firmin DN. Comparison of spiral and FLASH phase velocity mapping, with and without breath-holding, for the assessment of left and right coronary artery blood flow velocity. J Magn Reson Imaging 2004;19:40–49. [PubMed: 14696219]

Langerak SE, Vliegen HW, Jukema JW, Kunz P, Zwinderman AH, Lamb HJ, van der Wall EE, de Roos A. Value of magnetic resonance imaging for the noninvasive detection of stenosis in coronary artery bypass grafts and recipient coronary arteries. Circulation 2003;107:1502–1508. [PubMed: 12654607]

Lotz J, Doker R, Noeske R, Schuttert M, Felix R, Galanski M, Gutberlet M, Meyer GP. In vitro validation of phase-contrast flow measurements at 3 T in comparison to 1.5 T: precision, accuracy, and signal-to-noise ratios. J Magn Reson Imaging 2005;21:604–610. [PubMed: 15834905]

Marcus JT, Smeenk HG, Kuijer JP, Van der Geest RJ, Heethaar RM, Van Rossum AC. Flow profiles in the left anterior descending and the right coronary artery assessed by MR velocity quantification: effects of through-plane and in-plane motion of the heart. J Comput Assist Tomogr 1999;23:567–576. [PubMed: 10433289]

Markl M, Alley MT, Pelc NJ. Balanced phase-contrast steady-state free precession (PC-SSFP): a novel technique for velocity encoding by gradient inversion. Magn Reson 2003;49:945–952.

Markl M, Harloff A, Bley TA, Zaitsev M, Jung B, Weigang E, Langer M, Hennig J, Frydrychowicz A. Time-resolved 3D MR velocity mapping at 3T: improved navigator-gated assessment of vascular anatomy and blood flow. J Magn Reson Imaging 2007;25:824–831. [PubMed: 17345635]

Oshinski JN, Hofland L, Mukundan S, et al. Two-Dimensional MR Angiography of the Coronary Arteries without Breath-holding. Radiology 1996;201:737–743. [PubMed: 8939224]

Pelc NJ, Herfkens RJ, Shimakawa A, Enzmann DR. Phase contrast cine magnetic resonance imaging. Magn Reson Q 1991;7:229–254. [PubMed: 1790111]

Perktold K, Hofer M, Rappitsch G, Loew M, Kuban BD, Friedman MH. Validated computation of physiologic flow in a realistic coronary artery branch. J Biomech 1998;31:217–228. [PubMed: 9645536]

Pivkin IV, Richardson PD, Laidlaw DH, Karniadakis GE. Combined effects of pulsatile flow and dynamic curvature on wall shear stress in a coronary artery bifurcation model. J Biomech 2005;38:1283–1290. [PubMed: 15863113]

Prosi M, Perktold K, Ding Z, Friedman MH. Influence of curvature dynamics on pulsatile coronary artery flow in a realistic bifurcation model. J Biomech 2004;37:1767–1775. [PubMed: 15388320]

Ramaswamy SD, Vigmostad SC, Wahle A, Lai YG, Olszewski ME, Braddy KC, Brennan TM, Rossen JD, Sonka M, Chandran KB. Fluid dynamic analysis in a human left anterior descending coronary artery with arterial motion. Ann Biomed Eng 2004;32:1628–1641. [PubMed: 15675676]

Rebergen SA, van der Wall EE, Doornbos J, de Roos A. Magnetic resonance measurement of velocity and flow: technique, validation, and cardiovascular applications. Am Heart J 1993;126:1439–1456. [PubMed: 8249802]

Schiemann M, Bakhtiary F, Hietschold V, Koch A, Esmaeili A, Ackermann H, Moritz A, Vogl TJ, Abolmaali ND. MR-based coronary artery blood velocity measurements in patients without coronary artery disease. Eur Radiol 2006;16:1124–1130. [PubMed: 16411084]

Soulis JV, Farmakis TM, Giannoglou GD, Louridas GE. Wall shear stress in normal left coronary artery tree. J Biomech 2006;39:742–749. [PubMed: 16439244]

Tang C, Blatter DD, Parker DL. Accuracy of phase-contrast flow measurements in the presence of partial-volume effects. J Magn Reson Imaging 1993;3:377–385. [PubMed: 8448400]

van der Geest RJ, Niezen RA, van der Wall EE, de Roos A, Reiber JH. Automated measurement of volume flow in the ascending aorta using MR velocity maps: evaluation of inter- and intraobserver variability in healthy volunteers. J Comput Assist Tomogr 1998;22:904–911. [PubMed: 9843231]

Walker PG, Cranney GB, Scheidegger MB, Waseleski G, Pohost GM, Yoganathan AP. Semiautomated method for noise reduction and background phase error correction in MR phase velocity data. J Magn Reson Imaging 1993;3:521–530. [PubMed: 8324312]

Wang Y, Riederer SJ, Ehman RL. Respiratory motion of the heart: kinematics and the implications for the spatial resolution in coronary imaging. Magn Reson Med 1995;33:713–719. [PubMed: 7596276]

Weber OM, Martin AJ, Higgins CB. Whole-heart steady-state free precession coronary artery magnetic resonance angiography. Magn Reson Med 2003;50:1223–1228. [PubMed: 14648570]

Wittlinger T, Martinovic I, Noeske R, Moosdorf R, Lehmann F. High-field MR angiography on an in vitro stenosis model determination of the spatial resolution on 1.5 and 3T in correlation to flow velocity and contrast medium concentration. J Cardiovasc Magn Reson 2005;7:623–630. [PubMed: 16136851]

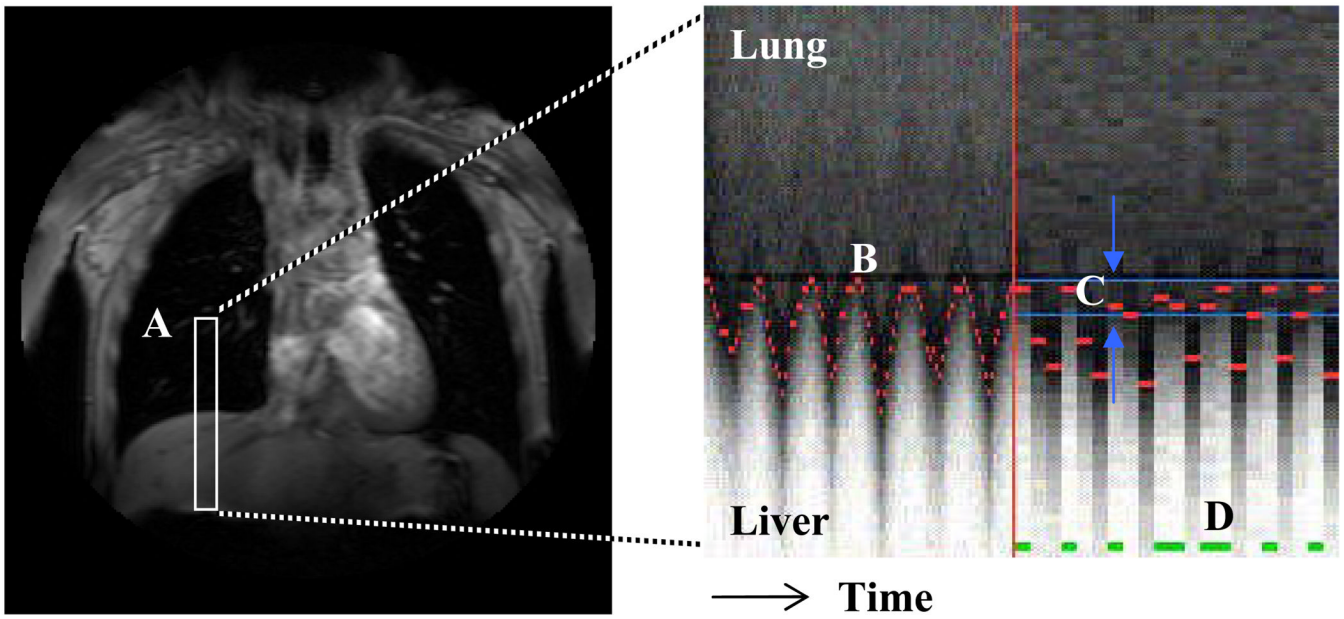

Figure 1.
A one-dimensional navigator-echo pulse (A, in white) is positioned over the liver and right lung to track the motion of the diaphragm over time. The boundary between the hypo-intense lung and hyper-intense liver at each heartbeat is recognized and tracked over time (B, in red). An acceptance window is defined at end respiration (C, in blue) and scan data is acquired for heartbeats during which the diaphragm lies within the acceptance window (D, in green).

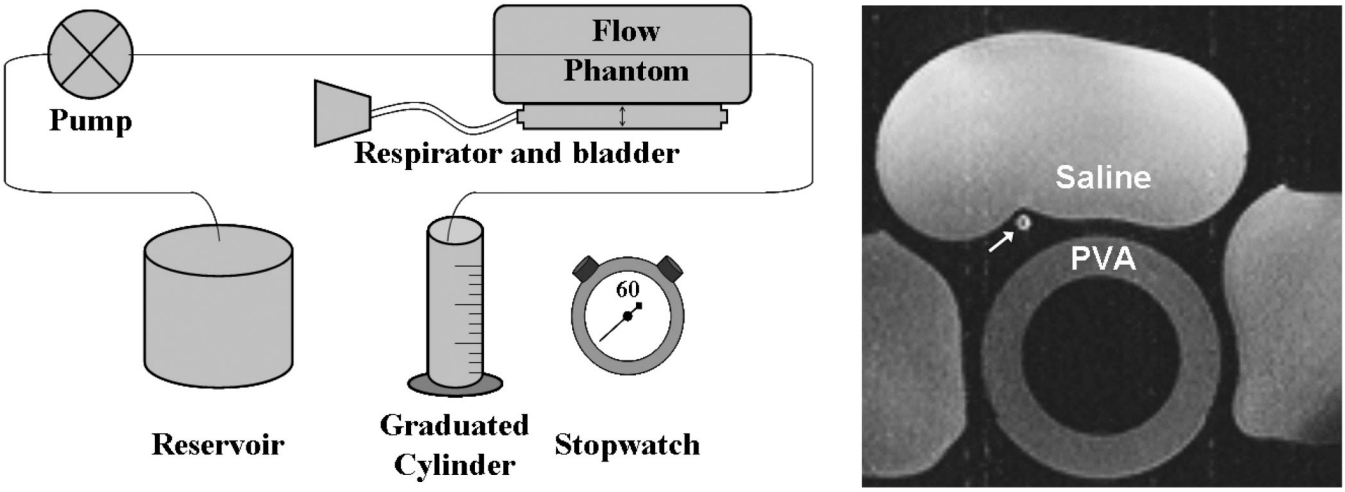

Figure 2.
Schematic of phantom flow setup consisting of a programmable flow pump, vessel phantom resting atop respiratory bladder, and graduated cylinder for timed collection of flow. A axial image of the *in vitro* setup shows the phantom vessel in cross-section (white arrow) as well as saline bags and PVA phantom.

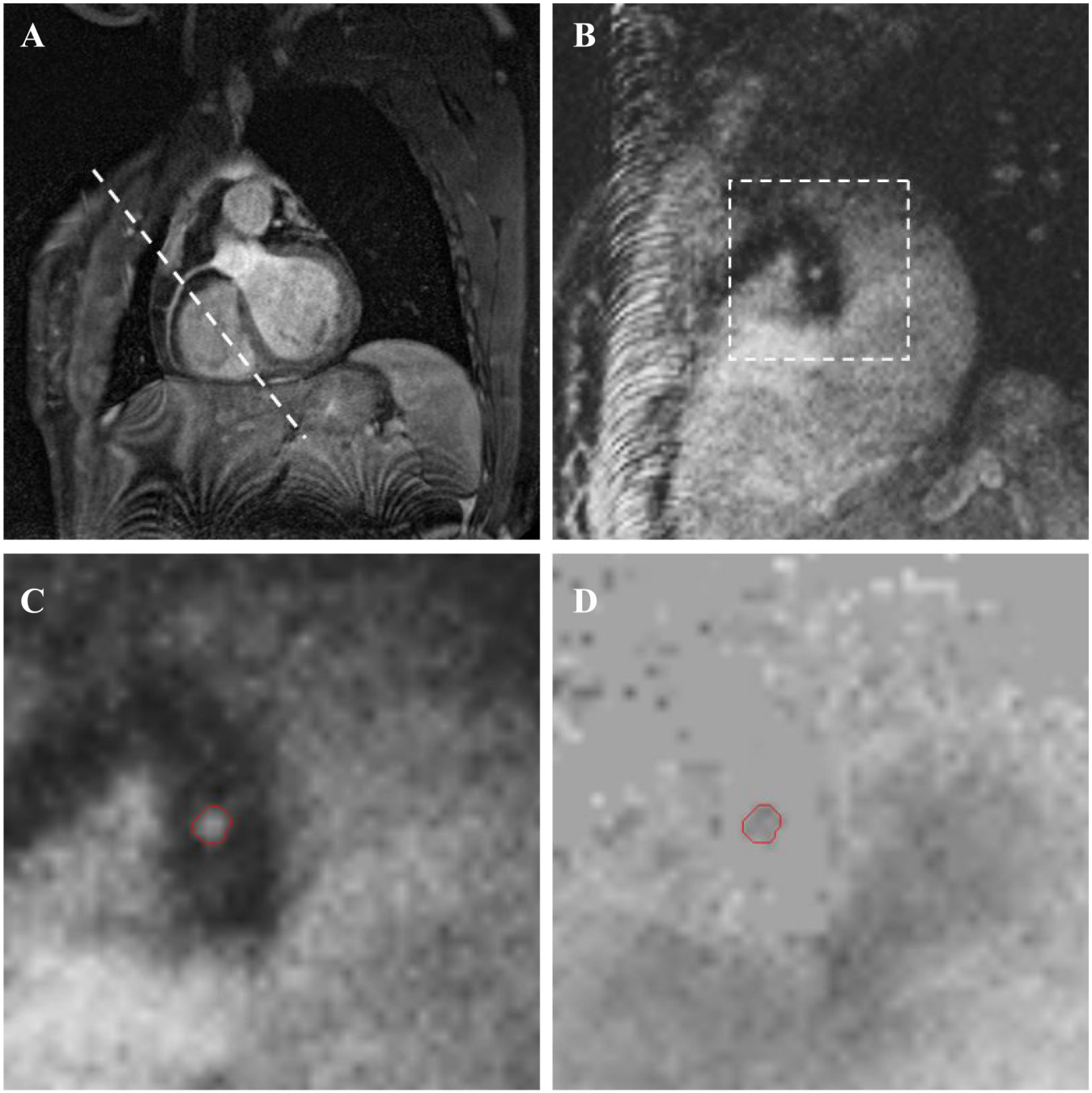

Figure 3.
Abbreviated *in vivo* MR protocol showing oblique slice of an in-plane RCA (A) with slice plane for the PC-MRI sequence (B). Zoomed views of the modulus (C) and phase (D) images from the PC-MRI scan show the ROI used to calculate velocity. Tissue surrounding the artery is nulled in the phase image by a filter based on low signal in the modulus image.

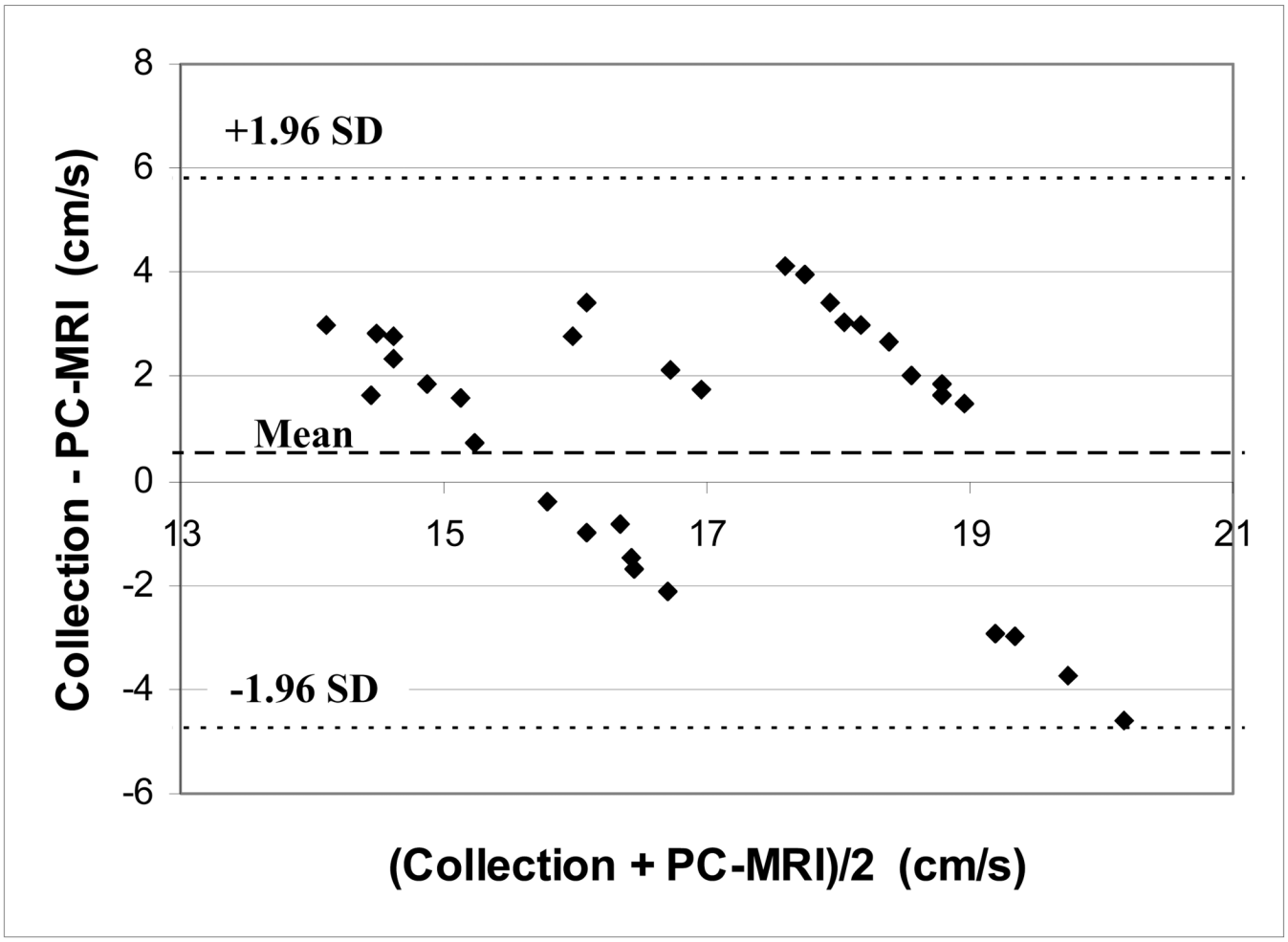

Figure 4.
Bland-Altman analysis of *in vitro* PC-MRI velocity measurements showing a mean difference of 0.5 cm/s and 95% confidence interval of [−4.8, 5.8] cm/s.

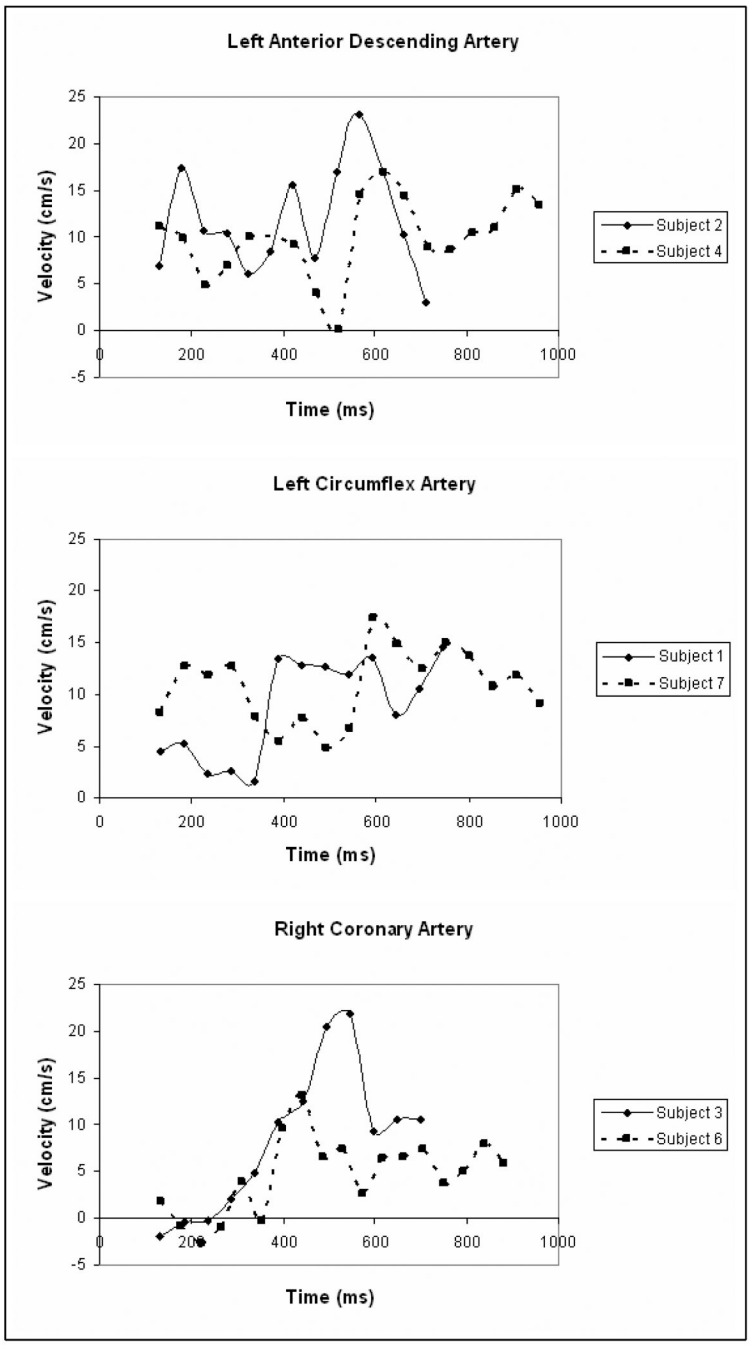

Figure 5.
Blood flow velocity curves in the LAD, LCX, and RCA of healthy volunteers. Multiple subjects are shown to illustrate intersubject variance in pattern and amplitude of velocity curves. Varying length of the curves reflect different heart rates of the subjects. The prospective, navigator echo gating pulse precludes data acquisition over the first 132ms of the cardiac cycle.

Table 1

Comparison of flow velocities measured by PC-MR and timed collection through 4mm tube.

Collected Flow Measurement mean ± SD (mL/s | cm/s)		PC-MR Flow Calculation mean ± SD (mL/s | cm/s)		RMS Error (%)
1.97 ± 0.02	15.7 ± 0.2 (n=14)	1.89 ± 0.23	15.0 ± 1.8	12%
2.23 ± 0.02	17.7 ± 0.2 (n=8)	2.30 ± 0.43	18.3 ± 3.4	18%
2.48 ± 0.01	19.7 ± 0.1 (n=14)	2.36 ± 0.39	18.8 ± 3.1	16%
				15%